Astronomy Letters, Vol. 29, No. 8, 2003, pp. 502–509. Translated from Pis'ma v Astronomicheskiĭ Zhurnal, Vol. 29, No. 8, 2003, pp. 571–579.

On the Mechanism of X-ray Emission from Radio Pulsars

I. F. Malov*

Pushchino Radio Astronomy Observatory, Astrospace Center, Lebedev Institute of Physics, Russian Academy of Sciences, Pushchino, Moscow oblast, 142290 Russia

Received February 10, 2003

Abstract—We discuss the correlations between the luminosities of radio pulsars in various frequency ranges and the magnetic fields on the light cylinder. These correlations suggest that the observed emission is generated in outer layers of the pulsar magnetospheres by the synchrotron mechanism. To calculate the distribution functions of the relativistic particles in the generation region, we use a model of quasi-linear interactions between the waves excited by cyclotron instability and particles of the primary beam and the secondary electron–positron plasma. We derive a formula for calculating the X-ray luminosity L_x of radio pulsars. A strong correlation was found between L_x and the parameter $\dot{P}_{-15}/P^{3.5}$, where P is the neutron-star rotation period, in close agreement with this formula. The latter makes it possible to predict the detection of X-ray emission from more than a hundred (114) known radio pulsars. We show that the Lorentz factors of the secondary particles are small ($\gamma_p = 1.5$–8.5), implying that the magnetic field near the neutron-star surface in these objects is multipolar. It follows from our model that almost all of the millisecond pulsars must emit X-ray synchrotron radiation. This conclusion differs from predictions of other models and can be used to test the theory under consideration. The list of potential X-ray radiators presented here can be used to search for X-ray sources with existing instruments.

Key words: *pulsars, neutron stars, and black holes; X-ray sources.*

1. INTRODUCTION

By now, X-ray emission from 41 radio pulsars has been detected by space telescopes (Possenti *et al.* 2002). Many attempts have been made to find correlations between the X-ray luminosities L_x and other parameters of these objects. In particular, a positive correlation was found between L_x and the rate of rotational energy losses $\dot{E}_r = I\Omega\dot{\Omega}$ (Becker and Trümper 1997). Here, Ω is the angular velocity of the neutron star and I is its moment of inertia. Malov and Malov (1995) showed that the integrated radio luminosity of the pulsars L_r also increased with increasing $\dot{E}_r$ ($L_r \propto \dot{E}_r^{1/3} \propto \dot{P}^{1/3}P^{-1}$). Such correlations seem quite natural, because the rotational energy of radio pulsars is believed to be the primary energy source for all types of their emission, although the exact dependence of L on $\dot{E}_r$ is still unknown. Thus, Possenti *et al.* (2002) showed that $L_x \propto \dot{E}^{1.34} \propto \dot{P}^{1.34}P^{-4}$. The dependence $L(\dot{E}_r)$ will probably differ for different samples, and we will not consider it below.

There are two points of view on the localization of the region where the X-ray emission of radio pulsars is generated. One group of authors (e.g., Zhang and Harding 2000) believe that this region is located in the acceleration zone, near the neutron-star surface. Other authors (e.g., Romani and Yadigaroglu 1994) assume that the hard (X-ray and gamma-ray) emission originates in the outer gap, on the periphery of the magnetosphere. In our papers (Malov and Machabeli 1999, 2001, 2002; Malov 2001b), we showed that the optical and X-ray emissions of radio pulsars must be generated in the outer layers of the magnetosphere, near the light cylinder, and there is no need to postulate an outer gap and an additional acceleration of relativistic particles.

Here, we once again discuss arguments for the generation of hard emission at large distances from the surface of a neutron star by the synchrotron mechanism (Section 2) and describe our synchrotron model (Section 3). Subsequently, we consider the possibilities for detecting X-ray emission from a number of known radio pulsars (Section 4) and summarize our main results (Section 5).

2. ARGUMENTS FOR THE SYNCHROTRON MODEL

Shortly after the detection of optical emission from the Crab pulsar, Shklovsky (1970) and Pacini (1971)

*E-mail: malov@prao.psn.ru

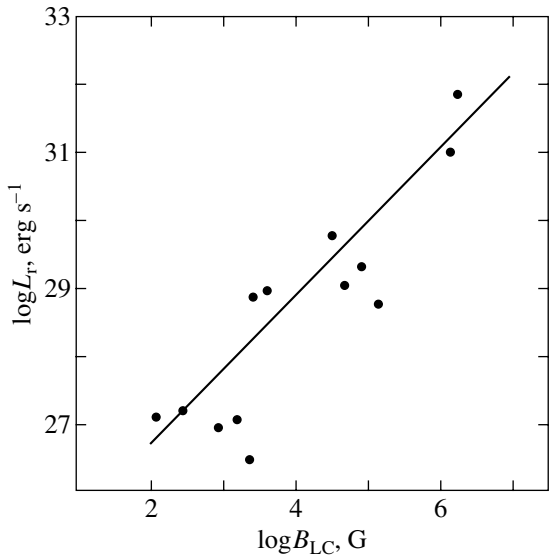

Fig. 1. The relationship between the radio luminosity of pulsars and the magnetic field at the light cylinder.

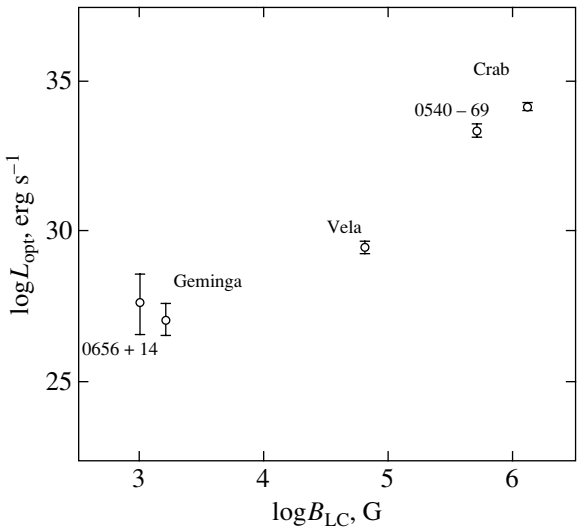

Fig. 2. The relationship between the optical luminosity of radio pulsars and the magnetic field $B_{\rm LC}$ (the diagram was taken from the paper of Shearer *et al.* 2000).

put forward the idea of using the synchrotron mechanism to explain this emission. They assumed that the generation region was located near the light cylinder ($r \sim R_{\rm LC} = c/\Omega$). Subsequently, a number of authors (Zheleznyakov 1971; Smith 1973; Ferguson 1981) suggested that the radiation from radio pulsars in all wavelength ranges was generated near the light cylinder. This extreme point of view was later transformed into the hypothesis of two types of pulsars (Malov and Suleymanova 1982; Malov 1987). Pulsars with long periods ($P = \Omega/2\pi \sim 1$ s) and with the generation of radio emission inside the magnetosphere at distances $r \ll R_{\rm LC}$ by the curvature radiation mechanism are objects of the first type. Pulsars with short periods ($P \lesssim 0.1$ s) belong to the second group of objects. The observed radiation is generated in these objects near the light cylinder by the synchrotron mechanism. Pulsars with intermediate periods can show properties characteristic of both types. There are various pieces of evidence for this division of radio pulsars (see, e.g., Malov 1997). However, in our view, the most convincing argument for this hypothesis is the high correlation between the integrated radio luminosity L_r and the magnetic field on the light cylinder $B_{\rm LC}$ (Malov 1999) (Fig. 1).

A strong argument for the generation of the entire observed emission in the same region is the similarity of the pulse profiles for the Crab pulsar PSR B0531+21 in all wavelength ranges, from radio to gamma rays (Smith 1977). Another argument for the localization of this region on the light cylinder is the high correlation between the optical luminosity of radio pulsars and the magnetic field $B_{\rm LC}$ (Shearer *et al.* 2000) (Fig. 2).

It is interesting to look at the dependence $L_x(B_{\rm LC})$. Using data for 41 pulsars (Possenti *et al.* 2002), we obtain the following relationship between L_x (2–10 keV) and $B_{\rm LC}$ (Fig. 3):

$$\log L_x(\mathrm{erg\ s^{-1}}) = (1.61 \pm 0.27) \log B_{\rm LC}(\mathrm{G}) + 24.94 \pm 1.25 \quad (1)$$

with the correlation coefficient $k = 0.69 \pm 0.12$. This correlation shows that the X-ray emission of radio pulsars is also generated near the light cylinder.

The calculations of the magnetic field at the light cylinder were carried out by assuming a dipole field structure in the entire pulsar magnetosphere:

$$B_{\rm LC} = B_s \left(\frac{R_*}{R_{\rm LC}}\right)^3 = \left(\frac{2\pi R_*}{c}\right)^3 \frac{B_s}{P^3}, \quad (2)$$

where R_* is the neutron-star radius, or for the magnetodipole model of neutron-star braking:

$$B_{\rm LC} = 5.9 \times 10^8 \left(\frac{\dot{P}}{P^5}\right)^{1/2} \mathrm{G}. \quad (3)$$

It should be emphasized that relation (1) must be corrected with an allowance made for two factors. First, it is necessary to subtract the part associated with the thermal radiation of the neutron-star surface from the observed flux to calculate the nonthermal (synchrotron) luminosity. Second, we should take into account the fact that the angles β between the rotation axes and the magnetic moments $\boldsymbol{\mu}$ of pulsars can be different. In this case, it is necessary to use $B = B_{\rm LC} \sin^3 \beta$ (Fig. 4) instead of $B_{\rm LC}$. It is hoped that an allowance for these two factors will lead to a

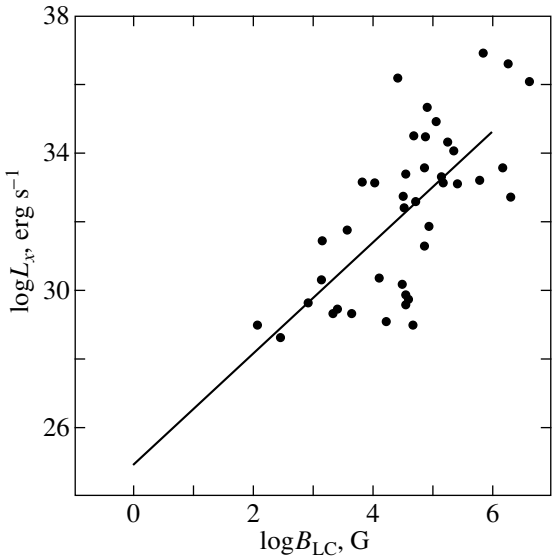

Fig. 3. The observed relationship between the X-ray luminosity of radio pulsars and the magnetic field at the light cylinder.

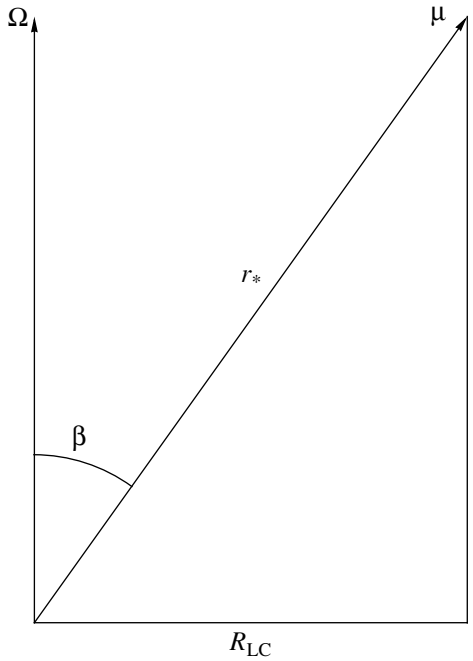

Fig. 4. The scheme to explain the decrease of the magnetic field strength in the generation region.

higher correlation between $\log L_x$ and $\log B_{\rm LC}$. Note that five radio pulsars with detected optical signals are simultaneously X-ray sources. This implies that their optical radiation is related to the tail of higher-energy emission, and the correlations $L_x(B_{\rm LC})$ and $L_{\rm opt}(B_{\rm LC})$ may not be independent.

The relationships shown in Figs. 1–3 allow us to use the synchrotron model to explain the observational data. This model is described in the next section.

3. DESCRIPTION OF THE MODEL

The total power of the synchrotron radiation emitted by a single electron is given by the expression (Pacholczyk 1970)

$$p = \frac{2e^4 B^2 \gamma^2 \sin^2\psi}{3m^2c^3}. \qquad (4)$$

Therefore, the synchrotron luminosity of any object depends on the distribution of the emitting particles in energy ϵ (or Lorentz factor $\gamma = \epsilon/mc^2$), on their pitch angles ψ (the angle between the particle velocity and the magnetic field), and on the magnetic field strength in the region where the radiation is generated. The distribution function shown in Fig. 5 is formed near the neutron-star surface (Arons 1981).

Here, $\gamma_{\rm b}$ characterizes the primary beam, and $\gamma_{\rm p}$ and $\gamma_{\rm t}$ characterize the secondary plasma. This function is one-dimensional, because any transverse momentum is lost by synchrotron radiation in less than 10^{-15} s. However, an anisotropic plasma is unstable (Sagdeev and Shafranov 1960) and certain types of waves will be excited. Their interaction with particles can give rise to appreciable pitch angles of the particles at sufficiently large distances from the neutron-star surface. Malov and Machabeli (2002) analyzed the steady-state kinetic equation

$$\frac{\partial}{\partial p_{||}}\left\{\left[\alpha_s\psi_0^2\left(\frac{p_{||}}{mc}\right)^2 + \alpha_c\left(\frac{p_{||}}{mc}\right)^4 - 2\pi^2\psi_0\frac{mc}{p_{||}}r_e\omega_k n_k\right]\mathrm{f}_{||}\right\} = 0, \qquad (5)$$

where $\alpha_s = 2e^2\omega_B^2/(3c^2)$, $\alpha_c = 2e^2/(3\rho^2)$, ρ is the radius of curvature of the magnetic field lines, $\omega_B = eB/(mc)$ is the cyclotron frequency, n_k is the number of plasmons, and $r_e = e^2/(mc^2)$ is the electron radius. They took into account the quasi-linear diffusion and the braking forces produced by the synchrotron and curvature radiations.

The solution of Eq. (5) can be sought in the form

$$\mathrm{f}(\mathbf{p}) = \chi(\psi)f(p).$$

If the cyclotron resonance is associated with the beam particles, then the distribution functions are

$$\chi(\psi) = C_1 e^{-A_1\psi^2}, \quad f_{||} \propto \gamma^{-4}. \qquad (6)$$

If the particles of the high-energy tail of the secondary-plasma distribution play a leading role, then the corresponding distribution functions at large distances from the neutron-star surface will be

$$\chi(\psi) = C_2 e^{-A_2\psi^4}, \qquad (7)$$

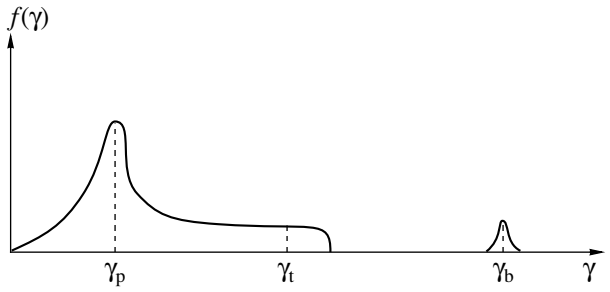

Fig. 5. The distribution function of relativistic particles in the pulsar magnetosphere.

$$f_{||}^{(1)} \propto \gamma, \quad f_{||}^{(2)} \propto \gamma^{-2}. \tag{8}$$

In formulas (6) and (7), A_1, A_2, C_1, and C_2 are constants. These distributions make it possible to calculate the synchrotron spectra. In particular, if $\gamma_b \sim 10^6$, $\gamma_p \sim 10$, and $\gamma_t \sim 10^5$, then the maximum frequency for PSR B0656+14 should be 7.5×10^{16} Hz ($\sim$0.5 keV) (Malov and Machabeli 2002), which is consistent with observations (Koptsevich *et al.* 2001). According to dependence (8), the intensity slowly decreases at high frequencies as $\nu^{-0.5}$.

Malov and Machabeli (2002) gave a formula for the synchrotron luminosity of radio pulsars:

$$L = \frac{\pi^2 e^4 I \gamma_r \dot{P} \psi^2 B^2}{4m^3 c^5 P^2}, \tag{9}$$

where γ_r is the Lorenz factor of the resonant particles. Here, we assume that the synchrotron radiation emanates from the part of the torus that is on the light cylinder and that one-half of the rotational energy losses is transferred by emitting particles. The high-energy tail particles ($\gamma_r = \gamma_t$) mainly contribute to the luminosity, and much of the radiation is emitted in the X-ray range. In this case, the mean Lorentz factor can be estimated from distribution (7); for

$$A_2 = \frac{4e^6}{3\pi^3 m^5 c^7} \frac{B^4 P^3 \gamma_p^4 \gamma_r^2}{\gamma_b^3}$$

it is equal to (Malov and Machabeli 2002)

$$\psi_0 \approx \frac{1}{2} \left(\frac{3\pi^3 m^5 c^7 \gamma_b^3}{4e^6 B^4 P^3 \gamma_p^4 \gamma_r^2} \right)^{1/4}. \tag{10}$$

The total luminosity can be calculated using the formula

$$L = \frac{\sqrt{3}}{32} \frac{\pi^{7/2} e I \dot{P} \gamma_b^{3/2}}{m^{1/2} c^{3/2} P^{7/2} \gamma_p^2}. \tag{11}$$

The first detailed model of synchrotron radiation from a radio pulsar was developed by Zheleznyakov and Shaposhnikov (1972) for PSR B0531+21. This model was critically analyzed in our other papers (see, e.g., Malov and Machabeli 2001). Here, we only emphasize that these and other investigators of the synchrotron model arbitrarily assumed the pitch angle to be $\psi \sim 1$. However, $\psi \ll 1$ in the magnetospheres of pulsars (including PSR B0531+21) (Machabeli and Usov 1989; Malov and Machabeli 2001). Indeed, if $\gamma_b = 10^6$, $\gamma_p = 10$, $\gamma_t = 10^5$, $P = 0.1$ s, and $r = R_{LC}$, then $\psi_0 \sim 10^{-3}$.

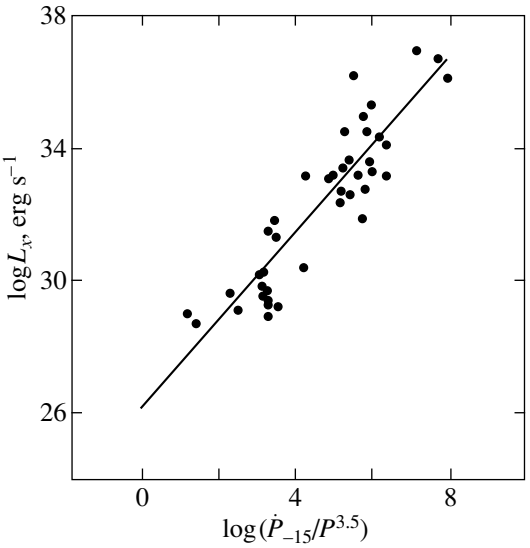

Fig. 6. The observed dependence of the X-ray luminosity of radio pulsars on the parameter $\dot{P}/P^{3.5}$.

Formula (11) makes it possible to relate the measured X-ray luminosity of radio pulsars to the observed parameter $\dot{P}/P^{3.5}$ if we assume that $\gamma_b^{1.5}/\gamma_p^2 =$ const. A comparison of L_x and $\dot{P}/P^{3.5}$ for 41 radio pulsars gives (Fig. 6)

$$\log L_x = (1.32 \pm 0.10) \log \frac{\dot{P}_{-15}}{P^{7/2}} + 26.12 \pm 0.48 \tag{12}$$

with the correlation coefficient $k = 0.91 \pm 0.07$.

Dependence (11) describes the relationship between the X-ray luminosity and other parameters of radio pulsars more accurately than the correlation $L_x - B_{\rm LC}$ does. This relationship includes no magnetic field. This is a fortunate circumstance, because the magnetic field on the neutron-star surface B_s is estimated in the magnetodipole model, but it may be incorrect when there are other pulsar slowdown mechanisms (Malov 2001a, 2003). Our subsequent calculations are free from such an uncertainty. In addition, it is not necessary to take into account any difference in the angles β for different pulsars in our model.

The high correlation coefficient between L_x and $\dot{P}/P^{3.5}$ implies that the model under consideration is correct and that the contribution of thermal radiation to L_x is basically small.

4. APPLICATIONS AND PREDICTIONS

The coefficient at $\log \dot{P}/P^{3.5}$ in Eq. (12) slightly differs from unity. If we assume that it is exactly equal to one, then we can calculate the mean value of the parameter $\gamma_b^{1.5}/\gamma_p^2$ for 41 pulsars from relation (11):

$$\log L_x = \log A + \log \frac{\dot{P}_{-15}}{P^{7/2}}. \qquad (13)$$

The most probable value of $\log A = 27.6$ corresponds to the parameter

$$\frac{\gamma_{\rm b}^{3/2}}{\gamma_{\rm p}^2} = 4.37 \times 10^8. \qquad (14)$$

We obtain $\gamma_p = 1.5$–8.5 for $\gamma_b = 10^6$–10^7. Such Lorentz factors of the secondary plasma can be achieved if the magnetic field near the neutron-star surface has a nondipolar structure (Machabeli and Usov 1989). Indeed, if the radius of curvature of the magnetic field lines is small ($\rho \sim R_*$), then a large number of curvature and synchrotron photons are emitted by each primary electron and much more electron–positron pairs than in the case of a dipole magnetic field, for which $\rho \sim 10^8$ cm $\gg R_*$, are produced. Here, R_* is the neutron-star radius. Therefore, the mean energy (Lorentz factor) of the secondary particles in a multipole field ($\gamma_p \lesssim 10$) is lower than that for a dipole field ($\gamma_p \sim 10^3$).

The minimum X-ray flux F in the range 2–10 keV is 8×10^{-16} erg s^{-1} cm^{-2} for the sample of 41 pulsars under consideration. Using this value, we can predict the detection of X-ray emission from other radio pulsars in the catalogues of Taylor *et al.* (1995), Manchester *et al.* (2001), and Morris *et al.* (2002). We obtain from formulas (11) and (14)

$$F = \frac{L}{4\pi d^2} = \frac{\sqrt{3}\pi^{5/2} e I \dot{P} \gamma_{\rm b}^{3/2}}{128 m^{1/2} c^{3/2} P^{7/2} \gamma_{\rm p}^2 d^2} \qquad (15)$$

$$= 3.34 \times 10^{-17} \frac{\dot{P}_{-15}}{P^{7/2} d_{\rm kpc}^2},$$

which corresponds to the condition

$$\eta = \frac{\dot{P}_{-15}}{P^{7/2} d_{\rm kpc}^2} \geq 24. \qquad (16)$$

The table lists the pulsars for which condition (16) is satisfied. We see that one might expect X-ray emission to be detected from more than 100 objects with the current sensitivity. For completeness, we also included pulsars with measured X-ray fluxes (Possenti *et al.* 2002) in the table. They are marked by asterisks. The expected fluxes F were also calculated for them using formula (15). This formula makes it possible to predict the detection of X-ray emission from newly discovered radio pulsars using their periods, the derivatives of the periods, and the distances.

5. DISCUSSION AND CONCLUSIONS

The table shows that almost all of the known millisecond radio pulsars must be X-ray emitters. The very low values of $\dot{P}$ for these objects are offset by the smallness of the factor $P^{3.5}$. Zhang and Harding (2000) concluded that the pulsed X-ray emission from most of the millisecond pulsars had a thermal nature. Future observations of these sources will allow the choice of a correct model to be made.

Below, we summarize our main results.

(1) We gave several arguments for the synchrotron model of X-ray emission from radio pulsars. A correlation was found between the X-ray luminosity and the magnetic field on the light cylinder, suggesting the generation of X-ray emission from these objects near the light cylinder.

(2) We briefly described a model for the formation of the electron-distribution function. This model is based on a quasi-linear interaction of the waves excited by the cyclotron instability in the magnetosphere with particles of the primary beam and the tail of the secondary plasma. A formula was derived to calculate the X-ray luminosity L_x of radio pulsars.

(3) We found a high correlation between L_x and the parameter $\dot{P}_{-15}/P^{3.5}$ (the correlation coefficient is $k = 0.91 \pm 0.07$). This correlation makes it possible to predict the detection of an X-ray flux from known and newly discovered radio pulsars.

(4) We gave a list of 114 objects whose X-ray emission can be detected at the current instrument sensitivity. If the search is successful, the number of radio pulsars with measured X-ray fluxes will at least double.

(5) We showed that the Lorentz factors at the maximum of the secondary-plasma distribution function lie within a very narrow range, $\gamma_p = 1.5$–8.5. This result implies that the magnetic field near the neutron-star surface is multipolar.

(6) The suggested model can be tested by searching for the predicted X-ray fluxes from the radio pulsars listed in the paper. In particular, synchrotron X-ray radiation must be detected from most of the known millisecond pulsars. This prediction is a crucial test that makes it possible to discriminate between the model under consideration and the model

Table

No.	PSR	$\log\eta$	$-\log F$	No.	PSR	$\log\eta$	$-\log F$
1	J0024−0534	4.38	12.10	41*	J1119−6127	<3.57	<12.91
2*	J0030+0451	4.37	12.11	42*	J1124−5916	4.55	11.93
3	B0053+47	1.69	14.79	43	B1133+16	1.45	15.03
4*	B0114+58	<3.59	<12.89	44	B1133−55	1.62	14.86
5	B0136+57	2.09	14.39	45	J1138−6207	1.57	14.91
6*	J0205+6449	5.59	10.89	46	B1143−60	1.39	15.09
7*	J0218+4232	3.56	12.92	47	B1257+12	8.19	8.29
8*	B0355+54	2.84	13.64	48	B1259−63	3.65	12.83
9*	J0437−4715	2.52	13.96	49	J1301−6305	2.59	13.89
10	B0450+55	2.21	14.27	50	B1317−53	1.65	14.83
11*	B0531+21	7.21	9.27	51	B1336−64	1.61	14.87
12*	J0537−6910	4.63	11.85	52	B1338−62	3.03	13.45
13*	J0538+2817	3.02	13.46	53	B1356−60	2.39	14.09
14*	B0540−69	3.85	12.63	54	J1406−6121	2.17	14.31
15	B0540+23	2.22	14.26	55	J1412−6145	1.81	14.67
16	J0613−0200	3.20	13.28	56*	J1420−6048	5.40	11.08
17	B0611+22	2.14	14.34	57*	J1435−6100	1.43	15.05
18	J0631+1036	2.28	14.20	58	B1449−64	2.52	13.96
19*	B0633+17	4.85	11.63	59	B1508−57	1.78	14.70
20*	B0656+14	3.44	13.04	60*	B1509−58	4.77	11.71
21	J0729−1448	2.88	13.60	61	B1516+02A	1.98	14.50
22	B0740−28	3.39	13.09	62	J1530−5327	2.26	14.22
23*	J0751+1807	2.90	13.58	63	B1534+12	2.70	13.78
24*	B0823+26	2.04	14.44	64	B1535−56	1.63	14.85
25*	B0833−45	6.38	10.10	65	J1548−5607	2.03	14.45
26	J0901−4624	1.43	15.05	66	B1556−44	1.65	14.83
27	B0905−51	1.51	14.97	67	B1557−50	1.61	14.87
28	B0906−17	1.61	14.87	68	J1601−5335	2.48	14.00
29	B0906−49	2.94	13.54	69	B1607−52	2.56	13.92
30	B0919+06	<1.47	<15.01	70	B1610−50	3.19	13.29
31	J0940−5428	3.95	12.53	71*	J1617−5055	4.88	11.60
32*	B0950+08	3.29	13.19	72	B1620−26	3.24	13.24
33*	J1012+5307	3.71	12.77	73	B1634−45	2.57	13.91
34*	J1016−5819	2.22	14.26	74	J1640+2224	3.07	13.41
35*	J1024−0719	3.39	13.09	75	J1643−1224	<2.32	<14.16
36	J1045−4509	1.70	14.78	76	B1643−43	2.60	13.88
37*	B1046−58	4.21	12.27	77	B1702−19	2.31	14.17
38*	B1055−52	2.87	13.61	78*	B1706−44	4.92	11.56
39*	J1105−6107	3.71	12.77	79	J1713+0747	3.04	13.44
40	J1112−6103	<2.70	<13.78	80	B1718−35	1.73	14.75

Table (Contd.)

No.	PSR	$\log\eta$	$-\log F$	No.	PSR	$\log\eta$	$-\log F$
81	J1718−3825	3.25	13.23	119	J1839−0321	1.60	14.88
82	B1719−37	2.43	14.05	120	J1841−0348	2.93	13.55
83	J1723−3659	2.06	14.42	121	B1841− 05	1.48	15.00
84	B1727−33	3.67	12.81	122	B1842−04	2.00	14.48
85	J1730−2304	3.18	13.30	123	B1844−04	1.50	14.98
86	B1730−37	1.75	14.73	124*	J1846−0258	3.01	13.47
87	B1734−35	1.48	15.00	125	J1849−0317	1.45	15.03
88	B1736−29	1.60	14.88	126	J1853+0056	2.10	14.38
89	B1737−30	2.39	14.09	127*	B1853+01	3.29	13.19
90	J1737−3137	1.83	14.65	128	B1855+09	3.29	13.19
91	J1738−2955	1.98	14.50	129	J1900+0227	2.00	14.48
92	J1739−3023	3.29	13.19	130	J1908+0734	2.75	13.73
93	B1742−30	1.92	14.56	131	J1909+0912	2.01	14.47
94	J1743−3153	1.72	14.76	132	J1913+0832	1.93	14.55
95*	J1744−1134	4.11	12.37	133	J1913+1011	4.27	12.21
96	B1749−28	1.41	15.07	134	B1914+09	1.47	15.01
97	B1754−24	2.23	14.25	135	B1915+13	2.12	14.36
98*	B1757−24	3.87	12.61	136	B1916+14	1.69	14.79
99*	B1800−21	3.99	12.49	137	J1918+1541	2.25	14.23
100	B1802−07	1.43	15.05	138*	B1929+10	3.86	12.62
101	J1809−1917	4.06	12.42	139	B1930+22	2.72	13.76
102*	J1811−1926	4.02	12.46	140*	B1937+21	4.73	11.75
103	B1820−30A	3.65	12.83	141*	B1951+32	4.88	11.60
104	B1820−31	1.94	14.54	142	B1953+29	1.74	14.74
105*	B1821−19	1.82	14.66	143	B1957+20	4.63	11.85
106	B1821−24	4.53	11.95	144	J2010+2425	3.36	13.12
107	B1822−09	2.11	14.37	145	B2020+28	1.68	14.80
108	B1822−14	1.83	14.65	146	B2022+50	1.39	15.09
109*	B1823−13	4.13	12.35	147	J2043+2740	3.59	12.89
110	B1828−10	2.03	14.45	148	B2127+11E	2.41	14.07
111	J1828−1101	3.45	13.03	149	B2127+11F	1.89	14.59
112	B1830−08	3.20	13.28	150*	J2124−3358	4.39	12.09
113	B1832−06	1.80	14.68	151	J2229+2643	2.81	13.67
114	J1835−1020	1.76	14.72	152*	J2229+6114	5.44	11.04
115	J1837−0559	1.56	14.92	153	J2317+1439	2.45	14.03
116	J1837−0604	3.63	12.85	154	J2322+2057	3.32	13.16
117	B1838−04	1.94	14.54	155*	B2334+61	2.57	13.91
118	J1838−0453	1.70	14.78				

* Pulsars with measured X-ray fluxes (Possenti *et al*. 2002).

for the generation of X-ray emission from these objects by the thermal mechanism near the neutron-star surface.

ACKNOWLEDGMENTS

This work was supported in part by the Russian Foundation for Basic Research (project no. 03-02-16509) and the NSF (grant no. 00-98685). I am grateful to L.B. Potapova for help in preparing the materials for publication and to the referees for useful remarks.

REFERENCES

1. J. Arons, in *Proceedings of the International Summer School and Workshop on Plasma Physics,* Ed. by T. D. Guyenne (Eur. Space Agency, Paris, 1981), p. 273.
2. W. Becker and J. Trúmper, Astron. Astrophys. **326**, 682 (1997).
3. D. C. Ferguson, Comments Astrophys. **9**, 127 (1981).
4. A. B. Koptsevich, G. G. Pavlov, S. V. Zharikov, *et al.*, Astron. Astrophys. **370**, 1004 (2001).
5. G. Z. Machabeli and V. V. Usov, Pis'ma Astron. Zh. **15**, 910 (1989) [Sov. Astron. Lett. **15**, 393 (1989)].
6. I. F. Malov, Aust. J. Phys. **40**, 731 (1987).
7. I. F. Malov, Astron. Zh. **74**, 697 (1997) [Astron. Rep. **41**, 617 (1997)].
8. I. F. Malov, Astron. Zh. **76**, 825 (1999) [Astron. Rep. **43**, 727 (1999)].
9. I. F. Malov, Astron. Zh. **78**, 452 (2001a) [Astron. Rep. **45**, 389 (2001a)].
10. I. F. Malov, Astron. Zh. **78**, 990 (2001b) [Astron. Rep. **45**, 865 (2001b)].
11. I. F. Malov, Astron. Zh. (2003), in press.
12. I. F. Malov and O. I. Malov, Astron. Zh. **72**, 574 (1995) [Astron. Rep. **39**, 510 (1995)].
13. I. F. Malov and G. Z. Machabeli, Astron. Zh. **76**, 788 (1999) [Astron. Rep. **43**, 691 (1999)].
14. I. F. Malov and G. Z. Machabeli, Astrophys. J. **554**, 587 (2001).
15. I. F. Malov and G. Z. Machabeli, Astron. Zh. **79**, 755 (2002) [Astron. Rep. **46**, 684 (2002)].
16. I. F. Malov and S. A. Suleymanova, Astrofizika **18**, 65 (1982).
17. R. N. Manchester, A. G. Lyne, F. Camilo, *et al.*, Mon. Not. R. Astron. Soc. **328**, 17 (2001).
18. D. J. Morris, G. Hobbs, A. G. Lyne, *et al.*, astro-ph/0204238 (2002).
19. A. G. Pacholczyk, *Radio Astrophysics* (Freeman, San Francisco, 1970; Mir, Moscow, 1973).
20. F. Pacini, Astrophys. J. Lett. **163**, L17 (1971).
21. A. Possenti, R. Cerutti, M. Colpi, and S. Mereghetti, astro-ph/0109452 (2002).
22. R. W. Romani and I.-A. Jadigaroglu, Astrophys. J. **438**, 314 (1994).
23. R. S. Sagdeev and V. D. Shafranov, Zh. Éksp. Teor. Fiz. **39**, 181 (1960) [Sov. Phys. JETP **12**, 130 (1960)].
24. F. J. Smith, Nature **243**, 207 (1973).
25. F. G. Smith, *Pulsars* (Cambridge Univ. Press, Cambridge, UK, 1977; Mir, Moscow, 1979).
26. A. Shearer, A. Golden, and J. Beskin, in *IAU Colloq. No. 177: Pulsar Astronomy—2000 and Beyond,* Ed. by M. Kramer, N. Wex, and R. Wielebinski (Kluwer Acad., Dordrecht, 2000), p. 307.
27. I. S. Shklovsky, Astrophys. J. Lett. **159**, L77 (1970).
28. J. H. Taylor, R. N. Manchester, A. J. Lyne, and F. Camilo, unpublished work (1995).
29. B. Zhang and A. K. Harding, Astrophys. J. **532**, 1150 (2000).
30. V. V. Zheleznyakov, Astrophys. Space Sci. **13**, 27 (1971).
31. V. V. Zheleznyakov and V. E. Shaposhnikov, Astrophys. Space Sci. **18**, 141 (1972).

Translated by I. Malov